Environ. Sci. Technol. **2007**, *41,* 6627−6632

Inactivation of Bacteriophages via Photosensitization of Fullerol Nanoparticles

APPALA RAJU BADIREDDY,[†] ERNEST M. HOTZE,[*,‡] SHANKAR CHELLAM,[†,§] PEDRO ALVAREZ,[∥] AND MARK R. WIESNER[‡]

Department of Civil and Environmental Engineering and Department of Chemical and Biomolecular Engineering, University of Houston, Houston, Texas 77204-4003, Department of Civil and Environmental Engineering, Duke University, Durham, North Carolina 27708-0287, and Department of Civil and Environmental Engineering, Rice University, Houston, Texas 77251-1892

The production of two reactive oxygen species through UV photosensitization of polyhydroxylated fullerene (fullerol) is shown to enhance viral inactivation rates. The production of both singlet oxygen and superoxide by fullerol in the presence of UV light is confirmed via two unique methods: electron paramagnetic resonance and reduction of nitro blue tetrazolium. These findings build on previous results both in the area of fullerene photosensitization and in the area of fullerene impact on microfauna. Results showed that the first-order MS2 bacteriophage inactivation rate nearly doubled due to the presence of singlet oxygen and increased by 125% due to singlet oxygen and superoxide as compared to UVA illumination alone. When fullerol and NADH are present in solution, dark inactivation of viruses occurs at nearly the same rate as that produced by UVA illumination without nanoparticles. These results suggest a potential for fullerenes to impact virus populations in both natural and engineered systems ranging from surface waters to disinfection technologies for water and wastewater treatment.

Introduction

Several fullerenes have been shown to be photosensitizers, producing reactive oxygen species (ROS) such as singlet oxygen ($^1O_2$) and superoxide ($O_2^{\bullet-}$) (*1*−*5*). Data from the medical literature detail the ability of C_{60} and C_{70} fullerenes to cleave DNA and inactivate viruses and bacteria and kill tumor cells (*6*−*10*). We have previously suggested that the photocatalytic properties of fullerenes might be exploited as the basis for developing processes for oxidation and disinfection in water treatment (*5*). In addition, the implications of possible ROS generation by fullerene nanoparticles on human health and environmental systems are unknown and require further study (*11*). In this paper, we describe photosensitive ROS generation by a hydroxylated C_{60} fullerene (fullerol) and the subsequent inactivation of waterborne bacterial viruses. This inactivation is proposed to occur by type I and type II photosensitization pathways that generate superoxide and singlet oxygen, respectively (Figure 1) (*12*).

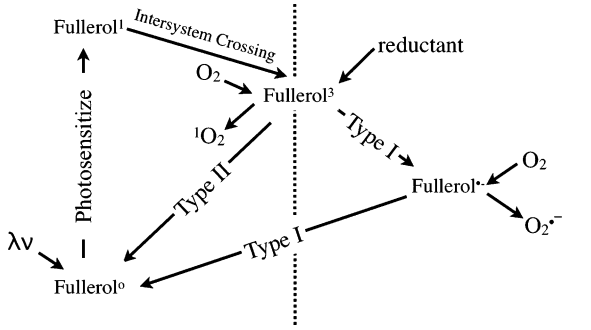

FIGURE 1. Proposed pathways of fullerol photosensitization via type I (right side of dotted line) and type II (left side of dotted line) resulting in superoxide and singlet oxygen, respectively.

The MS2 bacteriophage was chosen as a target for photosensitization for two reasons: the phage is principally employed for studies of water pollution and control (*13*−*19*) and it is similar in morphology to the hepatitis A virus and poliovirus. Significant inactivation of MS2 virus exceeds UVA (315−400 nm) irradiation alone when a fullerol suspension is present and shows that these nanoparticles could potentially impact microorganisms both in terms of environmental consequences and engineered water treatment. Moreover, we show that viral inactivation effectively serves as a probe for the presence of different ROS generated under both photocatalytic conditions and by the transfer of electrons from an appropriate donor.

Materials and Methods

Culture and Analysis of MS2 Phage. The double-top agar layer plaque technique was employed for MS2 (ATCC 15597-B1) propagation (*20*, *21*) using *Escherichia coli* (ATCC 15597) as the host. *E. coli* was first cultured for 18−24 h in a tryptic soy broth (TSB; Difco, Detroit, MI) and later transferred to fresh TSB and grown to a mid-log phase for 3−6 h at 37 °C. Stock MS2 was diluted in phosphate-buffered saline (PBS, composition 137 mM NaCl, 2.7 mM KCl, 4.3 mM $Na_2HPO_4 \cdot 7H_2O$, and 1.4 mM KH_2PO_4, pH 7.3) to a target concentration of 10^6 PFU/mL. Next, the *E. coli* suspension (0.9 mL) and phage dilution (0.1 mL) were mixed in 3 mL of soft overlay agar and poured onto presolidified trypticase soy agar (TSA, 1.5% agar; Difco, Detroit, MI) Petri dishes. Sterile PBS (6 mL) was then added to the Petri dishes, which resulted in confluent plaques after incubation for 24 h at 37 °C. The PBS solution containing the MS2 phages was decanted and centrifuged at 5000*g* for 10 min to remove bacterial debris. Additional purification of the fresh MS2 phages was achieved by filtering the supernatant through a track-etched ultrafiltration membrane rated at 80 nm (PCTE Nucleopore, Inc., Pleasanton, CA) and then ultra-centrifuging the filtrate (Beckman LB-70) at 103 000*g* for 3 h. The phage pellet was resuspended in PBS and stored at 4 °C. Fresh phage stock was prepared in this manner prior to each experiment.

MS2 samples from experiments were cultured using the method described previously. Following serial dilutions, plates were prepared in triplicate, and only plaques in the range of 30−300 were counted manually using a Scienceware colony counter (Bel-Art Products, Pequannock, NJ). Control

* Corresponding author phone: (919)660-5030; fax: 919-660-5219; e-mail: emh14@duke.edu.
† Department of Civil and Environmental Engineering, University of Houston.
‡ Duke University.
§ Department of Chemical and Biomolecular Engineering, University of Houston.
∥ Rice University.

10.1021/es0708215 CCC: $37.00
Published on Web 08/15/2007

experiments demonstrated that the viability of the MS2 host organism (*E. coli*) did not vary during the time scale of our experiments (see Supporting Information Table S1).

Chemicals. Superoxide dismutase (bovine erythrocytes) (SOD), 5,5-dimethyl-1-pyrroline-1-oxide (DMPO), 2,2,6,6-tetramethyl-4-piperidinol (4-oxo-TEMPO), adenosine 5′-(trihydrogen diphosphate) (NADH), 2,2,6,6-tetramethyl-4-piperidone (TEMP), nitro blue tetrazolium chloride (NBT), and β-carotene were obtained from Sigma-Aldrich (St. Louis, MO). Fullerol ($C_{60}(OH)_{22-24}$), was purchased from MER (Tucson, AZ). Deuterium oxide (D_2O) was purchased from Cambridge Isotope Laboratories (Andover, MA). Ultrapure water with a resistivity greater than 10 MΩ cm and dissolved organic carbon concentration <3 μg/L was autoclaved prior to use in all experiments. All glassware was washed with distilled water and autoclaved for 15 min.

Fullerol Suspension. Fullerol suspensions were made by adding approximately 0.07 mg/mL powdered fullerol to ultrapure water. This solution was made up in a volumetric flask and placed in a sonication bath for 2 h. During this time, the suspension became gradually more gold as more fullerol was suspended. Once removed from sonication, the suspension was filtered through 0.45 μm mixed cellulose easter (MCE) filters via vacuum to remove unsuspended particles. The final suspension of the fullerol aggregates had a number mean diameter of 218 nm and was found to be stable over a period of at least 3 months as determined by dynamic light scattering. Characteristics of the suspension have been previously published (*22*).

Irradiation and Inactivation Protocols. All experiments requiring irradiation were performed in the presence of two 15 W fluorescent ultraviolet bulbs (Philips TLD 15W/08). These bulbs had an output spectrum ranging from 310 to 400 nm and a total irradiance of 24.1 mW/m^2 with a peak at 365 nm in the UVA region as measured using a Li-Cor 1800 spectroradiometer (See Supporting Information Figure S1).

Two borosilicate glass vials with PTFE-lined caps were filled with 8 mL of a solution containing ~10^6 PFU/mL of the MS2 phage in PBS (pH 7.3 ± 0.1) and other necessary chemicals prior to irradiation at room temperature. One vial was exposed to UV irradiation, and the other was double-wrapped in aluminum foil, serving as a control sample. A reducing agent (5 mM NADH) was used to promote superoxide ($O_2^{\bullet-}$) formation, β-carotene (26 μM) was employed as a singlet oxygen ($^1O_2$) scavenger, and SOD (10 U/mL) was employed to scavenge $O_2^{\bullet-}$, depending on the specific experimental conditions. Viruses were sampled following 0, 5, 15, 30, 45, and 60 min of irradiation and enumerated using the plaque assay technique. Data points and error bars in each of the MS2 inactivation figures correspond to the mean and standard deviation of results from two or three separate experiments conducted under identical conditions on different dates over the duration of this study.

ROS Measurement Instrumentation. EPR spectra were recorded at room temperature with a Varian E-6 spectrometer. The conditions for all measurements were as follows: frequency, 9.27 GHz; power, 5 mW; modulation amplitude, 4 G; and modulation frequency, 100 kHz. UV−vis spectrometry was preformed using a Hitachi U-2000 spectrophotometer.

EPR Procedure. The spin-trapping reagent 4-oxo-TEMP was used to trap singlet oxygen (*23*). TEMP has a low detection limit and a relatively long adduct lifetime when compared to other spin traps, making it an ideal trap for suspensions containing low concentrations of singlet oxygen that must be irradiated for prolonged periods of time. To take a sample, a mixture of 40 μM fullerol suspension and 80 mM TEMP was shaken in a 5 mL volumetric flask. This was poured into a sample tray for UV irradiation. A portion of the sample was removed using a capillary tube, capped with clay, placed in a quartz EPR tube, and positioned in the EPR sample holder. The pH was controlled using PBS giving a pH of approximately 7.3. In each case, the EPR parameters were held constant as

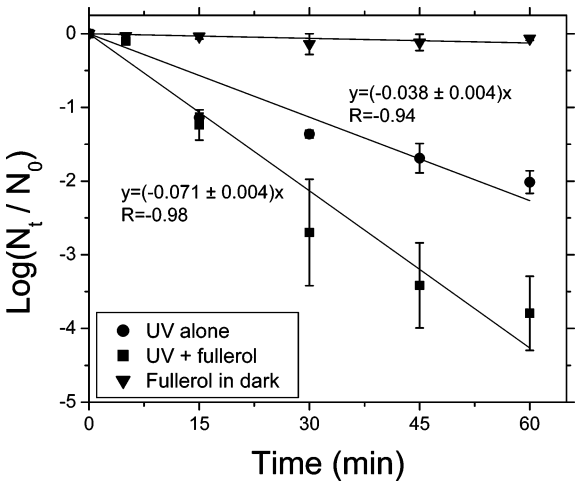

FIGURE 2. MS2 inactivation rate increases in the presence of 1 μM photoactivated fullerol. The same concentration of fullerol does not have an effect in the dark, while the rate of inactivation nearly doubles in the presence of UV and fullerol rather than UV alone. The best-fit value of the slope and the corresponding standard error are shown in all the graphs.

was the TEMP concentration. Separate samples were irradiated under UV for up to 3 h. Signals were compared with the standard product of TEMP and singlet oxygen (TEMPO) to determine the singlet oxygen generation rate (*6*).

Determination of Superoxide Concentrations by NBT Reduction. NBT reduction was employed to measure the production of superoxide (*24*). The reduction of NBT results in an increase in optical density that can be used to quantify the relative amount of superoxide present. The concentration of superoxide was determined by comparing NBT reduction with and without a quencher for superoxide, for which SOD allows non-superoxide related NBT reactions to be accounted. Samples were prepared by mixing two 10 mL flasks with the appropriate suspension and 625 μM NBT. One flask was kept free of SOD, and the other contained 10 U/mL SOD. These flasks were poured into four different 8 mL glass vials in 5 mL portions and capped with Teflon-lined septa. Four unique solutions resulted: suspension + UV, suspension + UV + SOD, suspension + DARK, and suspension + DARK + SOD. The former two provide a measure of superoxide activity under UV light, and the latter two provide a measure of superoxide activity in the dark. Light samples were irradiated for up to 60 min. A sample was taken via syringe at each time point. Dark samples were taken over the course of several hours while being stored in the refrigerator. All samples were analyzed for optical density at 560 nm, and the difference in optical density between the SOD-free and SOD-containing samples was taken to be proportional to the superoxide activity.

Results and Discussion

Results from several control experiments are summarized in the Supporting Information. In the absence of UV light, fullerol or controls with any of the added chemicals did not inactivate the MS2 host (*E. coli*) (Supporting Information Table S1), validating the plaque assay technique employed herein. Furthermore, none of the various chemical agents used in our experiment inactivated MS2 since no inactivation was observed in the absence of fullerol. However, MS2 was inactivated by photosensitized fullerol.

Inactivation with Fullerol in the Presence of UV Light. Figure 2 depicts MS2 inactivation under three scenarios: in the presence of UV radiation alone, UV sensitized fullerol, and fullerol in the dark. In all cases, inactivation could be closely approximated by first-order kinetics. The inactivation rate constant for MS2 by UVA irradiation alone was calculated

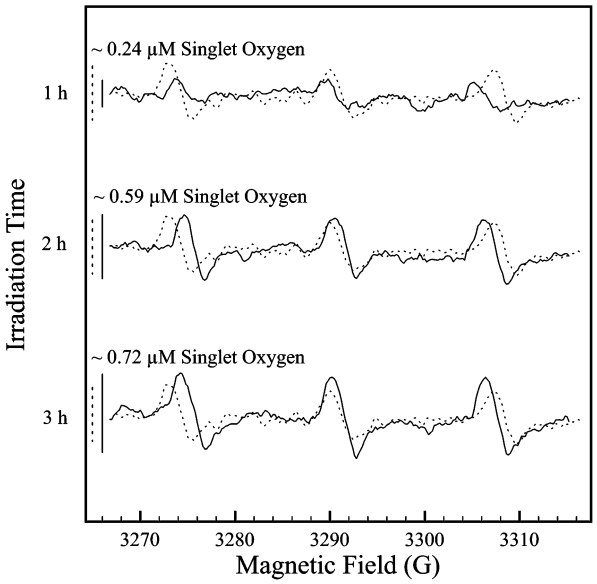

FIGURE 3. Electron paramagnetic resonance signal for 40 μM fullerol suspended in H_2O and containing PBS (pH 7.3). The suspension was irradiated for 1, 2, and 3 h. Triplet signal amplitude (black lines) can be compared with a 0.5 μM TEMPO standard (dotted lines) to find a detectible singlet oxygen generation rate.

to be 0.038 ± 0.004 min^{-1}. The inactivation rate increased significantly to 0.071 ± 0.004 min^{-1} when fullerol was added and the contents were exposed to UVA light. After 60 min of UV irradiation, the presence of fullerol increased MS2 inactivation to 4-log compared to 2-log of inactivation by UV alone. However, in the absence of UV light, fullerol produced negligible inactivation of MS2, with a disinfection rate constant that is statistically indistinguishable from zero. Enhanced inactivation of MS2 by UV in the presence of fullerol would therefore appear to be linked, in this case, with the ability of fullerol to act as a photosensitizer. Next, we explore the hypothesis that fullerol produced ROS in these viral inactivation experiments and evaluate the conditions that favor the production of various forms of ROS.

Previous work has shown that fullerol suspensions can produce ROS under conditions of acidic pH (*5*). Enhanced viral inactivation observed with fullerene and UV illumination in Figure 2 suggests that ROS was produced by fullerol at a near-neutral pH in our experiments. Subsequent data confirm the ROS production and speciation as either singlet oxygen or superoxide depending on the conditions of illumination and the presence of an electron donor.

Fullerol UV Irradiation Produces Singlet Oxygen. The two most likely ROS that caused increased virus inactivation are superoxide and singlet oxygen. Both species can be detected using EPR and an appropriate spin trap. TEMP was used to detect the singlet oxygen in Figure 3. In the presence of PBS, 40 μM fullerol, and MS2 virus, the triplet EPR signal grows after being irradiated for 1, 2, and 3 h. The constant and semilinear growth in the amplitude of the signal provides direct evidence that singlet oxygen is being generated by the fullerol suspension in the presence of UV light at a pH of 7.3. When either UV light or fullerol is absent, no signal is generated. These observations are consistent with the fact that there was no viral inactivation with fullerol in the dark under these conditions (Figure 2) and supports the hypothesis that photocatalytically produced singlet oxygen played a role in viral inactivation by fullerol.

These experiments were repeated using DMPO, a common spin trap for the detection of superoxide. No signal was generated in the presence of DMPO, an indication of negligible superoxide activity (data not shown).

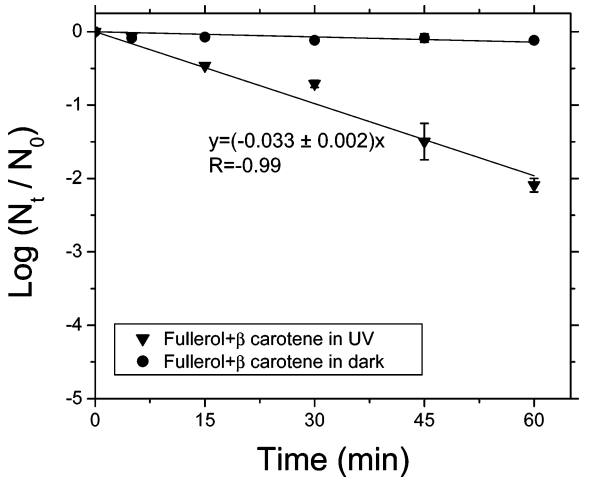

FIGURE 4. MS2 inactivation with photoactivated fullerol (1 μM) in the presence of β-carotene (26 μM). Inactivation is similar to that of UV alone (Figure 1).

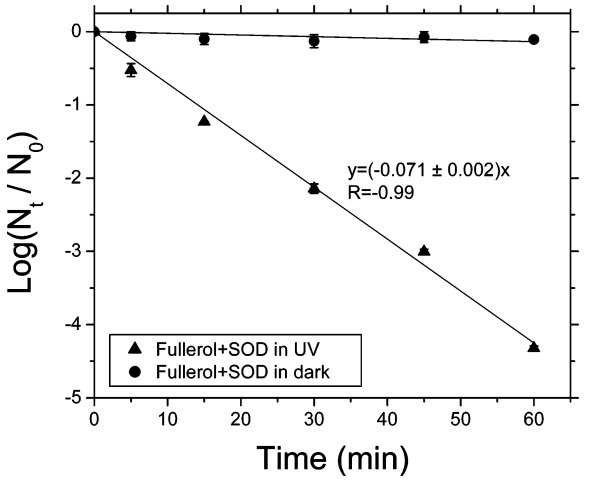

FIGURE 5. MS2 inactivation with photoactivated fullerol in the presence of SOD (10 U/mL). Inactivation is statistically indistinguishable to a similar suspension without SOD (Figure 2). (See Supporting Information for rate of inactivation of MS2 with SOD alone.)

Viral Sensitivity to Singlet Oxygen. Additional viral inactivation experiments were carried out in the presence of β-carotene and SOD (quenchers for singlet oxygen and superoxide, respectively) to further determine the ROS responsible for inactivation. Results from experiments conducted with fullerol in the presence of a singlet oxygen scavenger, β-carotene, are depicted in Figure 4. MS2 viruses were inactivated at a rate of 0.033 ± 0.002 min^{-1} when illuminated by UV light. This is statistically indistinguishable from the kinetics of inactivation obtained when the viruses were exposed to UV alone (0.038 ± 0.004 min^{-1} in Figure 2). As before, the dark inactivation rate was negligible and similar to that observed in Figure 2. Hence, additional MS2 inactivation by UV sensitized fullerol depicted in Figure 2 appears to result predominantly from singlet oxygen-mediated photooxidative stress. Negligible inactivation of MS2 was found when a suspension containing only β-carotene and NADH was irradiated (Table S2).

Inactivation experiments conducted in the presence of SOD (Figure 5) yielded MS2 inactivation rates that were statistically indistinguishable between UV sensitized fullerol in the presence or absence (Figure 2) of SOD (0.071 ± 0.002 min^{-1}). Thus, SOD addition did not influence MS2 inactivation kinetics, suggesting that photoactivated fullerol nano-

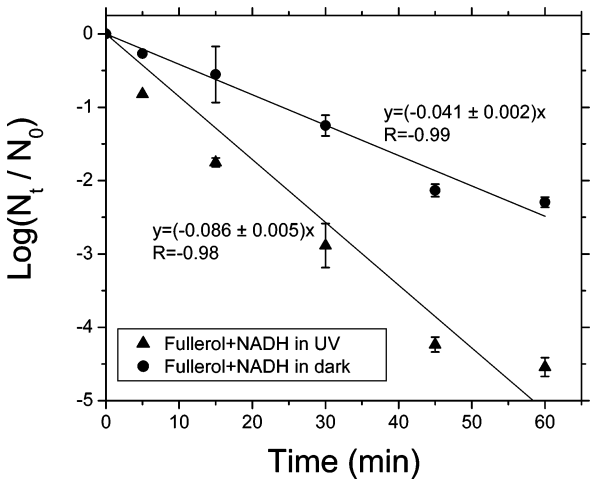

FIGURE 6. Increased MS2 inactivation with photoactivated fullerol (1 μM) in the presence of NADH (5 mM). (See Supporting Information for rate of inactivation of MS2 with NADH alone.)

particles either generated inconsequential amounts of superoxide or that superoxide contributed negligibly to MS2 inactivation. The latter explanation can be ruled out as superoxide is known to inactivate MS2 viruses (*25*). It is therefore reasonable to conclude that superoxide generation was negligible in these experiments and that the singlet oxygen produced photocatalytically by the fullerene was the primary agent of enhanced viral inactivation. Negligible inactivation of MS2 was found when a suspension containing only SOD was irradiated (Table S2).

Viral Sensitivity to Superoxide. Type I reactions that result in the production of superoxide require an appropriate electron donor to be present. NADH was chosen as an electron donor for two reasons: it is a biologically relevant donor found in the cell and had been used previously to study DNA cleavage by fullerene derivatives (*6*). The presence of NADH increased the rate of MS2 disinfection by UV sensitized fullerol to 0.086 ± 0.005 min^{-1} (Figure 6) from 0.071 ± 0.004 min^{-1} (Figure 2). These results suggest that in the presence of an electron donor (NADH), both singlet oxygen and superoxide radicals (generated simultaneously by type II and type I photosensitization) likely contributed to the higher MS2 inactivation rates by UVA sensitized fullerol.

Figure 6 also depicts substantial MS2 inactivation caused by fullerol and NADH together in the dark. The MS2 inactivation rate under these conditions is coincidentally similar to UVA alone (Figure 2) and is likely caused by superoxide production by fullerol in the presence of NADH. The high electron affinity of fullerenes suggests that ROS production might be possible in the dark when an appropriate electron donor is present. Negligible inactivation of MS2 was found when a suspension containing only NADH and bacteriophage was irradiated (Table S2). Unlike other reagents added in these experiments, NADH was observed to reduce the UV dose in this system. At the peak of irradiance (Figure S1), UV light transmission was reduced by over 50% when 5 mM NADH was present, and it is possible that fewer viruses were inactivated as a result. Therefore, the effect of the NADH−fullerol mixture may be even greater than that suggested in Figure 6 since the observed increase in inactivation rate with NADH likely represents a lower bound on the MS2 response. Despite this transmission reduction, NADH irradiated controls had no apparent deleterious effect on virus inactivation (Table S2).

Fullerol Generates Superoxide in the Presence of NADH. The production of superoxide via type II photosensitization (Figure 1) was evaluated in both the UV irradiated and the non-irradiated conditions utilizing an NBT absorbance measurement. When suspensions of fullerol were irradiated with UV in the presence of NADH, superoxide was produced as was measured by a change in the optical density at 560 nm (Table 1). Redox conditions favor the transfer of an electron from NADH (approximately −0.32 V vs SHE) to triplet fullerol (~0.958−0.851 V) (*1*, *2*). Some background production of superoxide by NADH was measured, but because the rate was 2.3 times higher in the presence of fullerol and no significant MS2 inactivation was measured with NADH alone (Table S2), viral inactivation may be attributed mainly to superoxide generation via type I photosensitization of fullerol. Consistently, no superoxide was produced by the fullerol suspension under UV irradiation in the absence of NADH (Table 1), consistent with a type II reaction (Figure 1) producing singlet oxygen as the main source of viral inactivation (Figure 2).

TABLE 1. Optical Density at 560 nm for NBT Reduced by Superoxide[a]

material	condition	time (h)	ΔOD (560 nm)
NADH	LP UV	1	0.56
Fullerol	LP UV	1	0.04
NADH + fullerol	LP UV	1	1.30
NADH	dark, 4 °C	96	0.19
Fullerol	dark, 4 °C	50	0.22
NADH + fullerol	dark, 4 °C	30	1.12
NADH + fullerol	dark, 4 °C	36	1.75
NADH + fullerol	dark, 4 °C	51	1.85

[a] Concentrations were 40 μM fullerol, 625 μM NBT, and 5 mM NADH in PBS. Vials were measured after being kept under LP UV exposure or in the dark at 4 °C over the time period indicated. Rate of superoxide production by fullerol/NADH was at least twice that of NADH alone in all cases.

Fullerol Generates Superoxide in the Dark. The same NBT reaction was used to probe superoxide production in samples without irradiation. The values of baseline differences in optical densities in SOD-containing solutions have been subtracted, leaving the optical density due to superoxide activity alone. Fullerol was not observed to produce superoxide in the dark when it was the only compound present in solution. In the dark, NADH alone has a very minimal superoxide producing power and consequently is only capable of limited viral inactivation (Table S2). However, when the suspension contained both NADH and fullerol, significant superoxide was produced in the dark (Table 1). We note, however, that estimated redox conditions do not seem to favor the transfer of an electron from NADH (approximately −0.32 V vs SHE) to ground state fullerol (approximately −0.602 V to −0.709 V) (*2*), suggesting that other solutes may play a role in mediating this reaction.

Dark and Light Superoxide Generation Is Confirmed by Quenchers. We further tested the hypothesis that the fullerol−NADH combination inactivated viruses by superoxide production in the dark by adding SOD to quench any superoxide produced under these conditions. In the presence of the SOD, a negligible virus inactivation in the dark was produced by the fullerol−NADH mixture (Figure 7), as is consistent with SOD effectively quenching the superoxide radicals. A photoactivated mixture of fullerol nanoparticles, NADH, and SOD gave lower virus inactivation rates (0.057 ± 0.004 min^{-1} in Figure 7) as compared to a mixture of photoactivated fullerol nanoparticles and NADH alone (0.086 ± 0.005 min^{-1} in Figure 7), suggesting that both singlet oxygen and superoxide are produced when fullerol is irradiated. The lower rate of inactivation produced by the photoactivated mixture of fullerol nanoparticles, NADH, and SOD (0.057 ± 0.004 min^{-1} in Figure 7) as compared to either the photoactivated fullerol alone (0.071 ± 0.004 min^{-1} in Figure 2) or the photoactivated fullerol with SOD (0.071 ± 0.002 min^{-1}

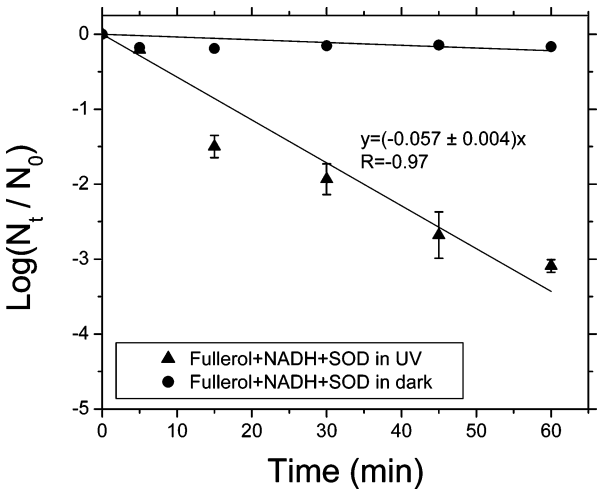

FIGURE 7. Effects of SOD (10 U/mL) addition to a suspension of fullerol (1 μM) and NADH (5 mM) on MS2 inactivation.

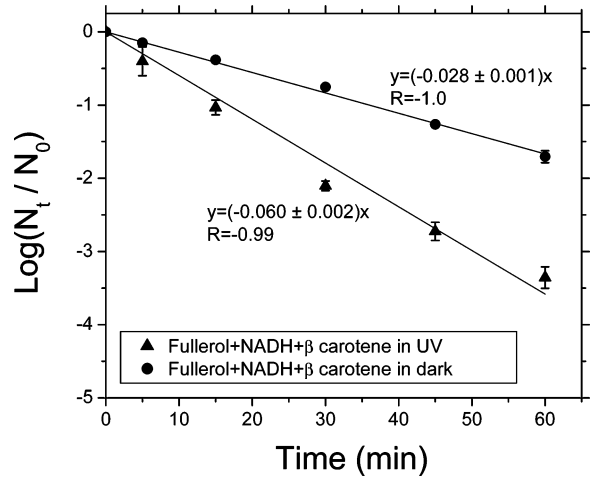

FIGURE 8. Effects of β-carotene (26 μM) addition to a suspension of fullerol and NADH (5 mM) on MS2 inactivation.

in Figure 5) may indicate that NADH may be competing with oxygen in the photosensitization reaction with the triplet state of fullerol resulting in lower levels of singlet oxygen production (Figure 1) or that NADH reduced transmission. Indeed, negligible inactivation rates of MS2 were found when a suspension containing only SOD and NADH was irradiated (Table S2).

In addition, viral inactivation rates for a UV illuminated system with fullerol, NADH, a superoxide promoter, and β-carotene, a singlet oxygen quencher (0.060 ± 0.002 min^{-1} in Figure 8), were greater than those observed for UV alone (0.038 ± 0.004 min^{-1} in Figure 2). This observation, combined with β-carotene quenching performed without NADH present (Figure 4), further implicates the superoxide radicals formed via type I photosensitization of fullerol as the likely inactivation agents for MS2 as it reduces the likelihood that superoxide is only generated from the direct transfer of electrons from NADH to singlet oxygen (*26*). If this were the case, UV plots in Figures 4 and 8 would match. Also, as depicted in Figure 8, the dark inactivation rate (0.028 ± 0.001 min^{-1}) was lower than that for conditions favoring superoxide alone (fullerol and NADH in the dark, 0.041 ± 0.002 min^{-1} in Figure 6), indicating possible crossover quenching of superoxide radicals by β-carotene. As suspected from the photosensitization theory, this further supports the hypothesis that singlet oxygen is not being produced by fullerol in the dark. Also, negligible inactivation of MS2 was found when a suspension containing only β-carotene and NADH was irradiated (Table S2).

These observations of ROS generation and subsequent viral inactivation by fullerol nanoparticle suspensions suggest both possible impacts on ecosystems and new water treatment technologies. Numerous hurdles must be addressed before these materials can be used in water treatment including the development of methods for immobilization or separation of nanomaterials, evaluation of long-term efficacy, and cost. Further investigations will be needed to determine if low levels of UV light incident upon a lake or river may result in ROS generation that may impact microorganisms, as well as an estimate of the quantities and format of these materials expected to be present in natural systems, before an assessment of the impact of these on natural systems can be performed.

Acknowledgments

This work was funded in part by the EPA-STAR Grant 91650901-0, a NSF Nano Exploratory Research Grant (BES-0508207), the Partnership in International Research and Education, the Nanoscale Science and Engineering Initiative of the NSF, a NSF CAREER award to S.C. (BES 0134301), and the EPA STAR program. The authors thank Fabian Marian of the Biochemistry Department at Rice University for his assistance with EPR spectra acquisition and analysis.

Supporting Information Available

Irradiance of low-pressure UV utilized in this study (Figure S1). Analysis of the viability of *E. coli* when exposed to fullerol suspensions alone and fullerol with NADH, SOD, or β-carotene (Table S1). Inactivation rates of MS2 phage when exposed to fullerol-free suspensions containing NADH, SOD, and β-carotene (Table S2). This material is available free of charge via the Internet at http://pubs.acs.org.

Literature Cited

(1) Arbogast, J. W.; Darmanyan, A. P.; Foote, C. S.; Rubin, Y.; Diederich, F. N.; Alvarez, M. M.; Anz, S. J.; Whetten, R. L. Photophysical Properties of C_{60}. *J. Phys. Chem.* **1991**, *95*, 11−12.

(2) Mohan, H.; Palit, D. K.; Mittal, J. P.; Chiang, L. Y.; Asmus, K. D.; Guldi, D. M. Excited states and electron transfer reactions of $C_{60}OH_{18}$ in aqueous solution. *J. Chem. Soc., Faraday Trans.* **1998**, *94*, 359−363.

(3) Hamano, T.; Okuda, K.; Mashino, T.; Hirobe, M.; Arakane, K.; Ryu, A.; Mashiko, S.; Nagano, T. Singlet oxygen production from fullerene derivatives: Effect of sequential functionalization of the fullerene core. *Chem. Commun.* **1997**, 21−22.

(4) Vileno, B.; Marcoux, P. R.; Lekka, M.; Sienkiewicz, A.; Feher, I.; Forro, L. Spectroscopic and photophysical properties of a highly derivatized C_{60} fullerol. *Adv. Funct. Mater.* **2006**, *16*, 120−128.

(5) Pickering, K. D.; Wiesner, M. R. Fullerol-sensitized production of reactive oxygen species in aqueous solution. *Environ. Sci. Technol.* **2005**, *39*, 1359−1365.

(6) Yamakoshi, Y.; Umezawa, N.; Ryu, A.; Arakane, K.; Miyata, N.; Goda, Y.; Masumizu, T.; Nagano, T. Active oxygen species generated from photoexcited fullerene (C_{60}) as potential medicines: $O_2^{\bullet -}$ versus $^1O_2$. *J. Am. Chem. Soc.* **2003**, *125*, 12803−12809.

(7) Kasermann, F.; Kempf, C. Photodynamic inactivation of enveloped viruses by buckminsterfullerene 1. *Antiviral Res.* **1997**, *34*, 65−70.

(8) Mashino, T.; Okuda, K.; Hirota, T.; Hirobe, M.; Nagano, T.; Mochizuki, M. Inhibition of *E. coli* growth by fullerene derivatives and inhibition mechanism. *Biorg. Med. Chem. Lett.* **1999**, *9*, 2959−2962.

(9) Tabata, Y.; Murakami, Y.; Ikada, Y. Antitumor effect of poly(ethylene glycol) modified fullerene. *Fullerene Sci. Technol.* **1997**, *5*, 989−1007.

(10) Tsao, N.; Luh, T.; Chou, C.; Wu, J.; Lin, Y.; Lei, K. Inhibition of group A *Streptococcus* infection by carboxyfullerene. *Antimicrob. Agents Chemother.* **2001**, *45*, 1788−1793.

(11) Wiesner, M. R; Lowry, G. V.; Alvarez, P.; Dionysiou, D.; Biswas, P. Assessing the risks of manufactured nanomaterials. *Environ. Sci. Technol.* **2006**, *40* (14), 4336−4345.

(12) Foote, C. S. Definition of type-I and type-II photosensitized Oxidation. *Photochem. Photobiol.* **1991**, *54*, 659−659.
(13) Ryan, J. N.; Harvey, R. W.; Metge, D.; Elimelech, M.; Navigato, T.; Pieper, A. P. Field and laboratory investigations of inactivation of viruses (PRD1 and MS2) attached to iron oxide-coated quartz sand. *Environ. Sci. Technol.* **2002**, *36*, 2403−2413.
(14) Jin, Y.; Yates, M. V.; Thompson, S. S.; Jury, W. A. Sorption of viruses during flow through saturated sand columns. *Environ. Sci. Technol.* **1997**, *31*, 548−555.
(15) Dowd, S. E.; Pillai, S. D.; Wang, S.; Corapcioglu, M. Y. Delineating the specific influence of virus isoelectric point and size on virus adsorption and transport through sandy soils. *Appl. Environ. Microbiol.* **1998**, *64*, 405−410.
(16) Gerba, C. P.; Bitton, G. Microbial pollutants: Their survival and transport pattern to groundwater. In *Groundwater Pollution Microbiology*; Bitton, G., Gerba, C. P., Eds.; John Wiley and Sons: New York, 1984; pp 65−88.
(17) Batch, L. F.; Schulz, C. R.; Linden, K. G. Evaluating water quality effects on UV disinfection of MS2 coliphage. *J. Am. Water Works Assoc.* **2004**, *96*, 75−87.
(18) Kohn, T.; Nelson, K. L. Sunlight-mediated inactivation of MS2 coliphage via exogenous singlet oxygen produced by sensitizers in natural waters. *Environ. Sci. Technol.* **2007**, *41*, 192−197.
(19) Mi, B.; Marinas, B. J.; Curl, J.; Sethi, S.; Crozes, G. Microbial passage in low pressure membrane elements with compromised integrity. *Environ. Sci. Technol.* **2005**, *39*, 4270−4279.
(20) Adams, M. H. *Bacteriophages*; Interscience Publishers, Inc.: New York, 1959.
(21) Meng, Q. S.; Gerba, C. P. Comparative inactivation of enteric adenoviruses, poliovirus, and coliphages by ultraviolet irradiation. *Water Res.* **1996**, *30*, 2665−2668.
(22) Xia, T.; Kovochich, M.; Brant, J.; Hotze, M.; Sempf, J.; Oberley, T.; Sioutas, C.; Yeh, J. I.; Wiesner, M. R.; Nel, A. E. Comparison of the abilities of ambient and manufactured nanoparticles to induce cellular toxicity according to an oxidative stress paradigm. *Nano Lett.* **2006**, *6*, 1794−1807.
(23) Lion, Y.; Delmelle, M.; Vandevorst, A. New method of detecting singlet oxygen production. *Nature (London, U.K.)* **1976**, *263*, 442−443.
(24) Bielski, B. H. J.; Shiue, G. G.; Bajuk, S. Reduction of nitro blue tetrazolium by CO^{2-} and O^{2-} radicals. *J. Phys. Chem.* **1980**, *84*, 830−833.
(25) Cho, M.; Chung, H.; Choi, W.; Yoon, J. Different inactivation behaviors of MS-2 phage and *Escherichia coli* in TiO_2 photocatalytic disinfection. *Appl. Environ. Microbiol.* **2005**, *71*, 270−275.
(26) Sparrow, J. R.; Vollmer-Snarr, H. R.; Zhou, J. L.; Jang, Y. P.; Jockusch, S.; Itagaki, Y.; Nakanishi, K. A2E-epoxide damaged DNA in retinal pigment epithelial cells: Vitamin E and other antioxidants inhibit A2E-epoxide formation. *J. Biol. Chem.* **2003**, *278*, 18207−18213.

Received for review April 6, 2007. Revised manuscript received June 15, 2007. Accepted July 9, 2007.

ES0708215